Petroleum Research 5 (2020) 202–209

Contents lists available at ScienceDirect

Petroleum Research

journal homepage: http://www.keaipublishing.com/en/journals/petroleum-research/

Reservoir and lithofacies shale classification based on NMR logging

Hongyan Yu [a, b, *], Zhenliang Wang [a], Fenggang Wen [c], Reza Rezaee [b], Maxim Lebedev [b], Xiaolong Li [a], Yihuai Zhang [d], Stefan Iglauer [e]

[a] State Key Laboratory of Continental Dynamics, National and Local Joint Engineering Research Center for Carbon Capture Utilization and Sequestration, Department of Geology, Northwest University, Xi'an, 710069, China
[b] WA School of Mines: Minerals, Energy and Chemical Engineering, Curtin University, 26 Dick Perry Avenue, 6151, Kensington, Australia
[c] Institute of Shaanxi Yanchang Petroleum Group Co.,Ltd, Xi'an, Shaanxi, 710075, China
[d] Department of Earth Science and Engineering, Imperial College London, London, SW7 2BP, United Kingdom
[e] Shool of Engineering, Edith Cowan University, 270 Joondalup Drive, WA, 6027, Australia

ARTICLE INFO

Article history:
Received 8 January 2020
Received in revised form
1 May 2020
Accepted 4 May 2020
Available online 10 May 2020

Keywords:
Shale gas
NMR logging
Pore size distribution
Composition

ABSTRACT

Shale gas reservoirs have fine-grained textures and high organic contents, leading to complex pore structures. Therefore, accurate well-log derived pore size distributions are difficult to acquire for this unconventional reservoir type, despite their importance. However, nuclear magnetic resonance (NMR) logging can in principle provide such information via hydrogen relaxation time measurements. Thus, in this paper, NMR response curves (of shale samples) were rigorously mathematically analyzed (with an Expectation Maximization algorithm) and categorized based on the NMR data and their geology, respectively. Thus the number of the NMR peaks, their relaxation times and amplitudes were analyzed to characterize pore size distributions and lithofacies. Seven pore size distribution classes were distinguished; these were verified independently with Pulsed-Neutron Spectrometry (PNS) well-log data. This study thus improves the interpretation of well log data in terms of pore structure and mineralogy of shale reservoirs, and consequently aids in the optimization of shale gas extraction from the subsurface.

1. Introduction

Nuclear magnetic resonance (NMR) is an effective tool to probe reservoir characteristics, including unconventional shale gas reservoirs. NMR can provide pore-scale – bound fluid porosity (Bauer et al., 2015), free fluid porosity and fracture porosity (Talabi et al., 2009), permeability (Kleinberg et al., 2003), hydrocarbon existence (Kapur et al., 2000), mineral composition (Cho et al., 2003) and fracture morphology (Pan et al., 2009). Typically, shale gas reservoirs display a complicated pore morphology (Chalmers et al., 2012; Yu et al., 2016, 2017a; Liu et al., 2018; Wang, 2018), and although laboratory NMR can obtain precise shale pore size distributions, yet it is still a challenge to continuously measure and interpret NMR data at well-log scale (Gallegos and Smith, 1988; Yao and Liu, 2012; Kenyon, 1997; Latorraca et al., 1999; Odusina and Sigal, 2011). Furthermore, laboratory NMR tests areconducted at centimetre scale and ambient conditions (Howard et al., 1995; Kamath et al., 1999), in contrast to NMR well logging tests which are conducted at decameter scale and wellboreconditions (Howard et al., 1995; Kamath et al., 1999). In this context, NMR logs, when compared to laboratory NMR experiments, providean opportunity to improve the analysis of in-situ well log data and consequently improved petrophysical property analysis. Thus in this study T_2time distributions from NMR logs were analyzed to obtain pore size distributions and pore properties for a shale gas reservoir. It was found that apart from bound fluid and free fluid porosity fractures play a crucial part in NMR spectrum. Expectation Maximization algorithm was used for clustering the different pore types in the reservoir, and based on the shape of the NMR spectra, seven lithological classes were identified. These were independently identified via pulsed neutron spectroscopy (PNS) to validate the NMR analysis proposed here. The classified sub-reservoirs show a good assess to fracturing and reservoir

* Corresponding author. State Key Laboratory of Continental Dynamics, National and Local Joint Engineering Research Center for Carbon Capture Utilization and Sequestration, Department of Geology, Northwest University, Xi'an, 710069, China.
E-mail addresses: amelia-yu@hotmail.com, yuhy@nwu.edu.cn (H. Yu).

https://doi.org/10.1016/j.ptlrs.2020.04.005

heterogeneity evaluation.

2. Background

2.1. Geological setting

The Shale gas reservoir of YanChang formation from south-eastern Ordos Basin, China (Fig. 1) is used as a shale gas reservoir example to investigate the newly proposed NMR log analysis. In the inland Ordos Basin, the YC formation (Upper Triassic) sediments are mostly deposited in fluvial and lacustrine sedimentary environments (Hongyan et al., 2016). One of the most important shale gas reservoirs in China in this formation was formed in deep and semi-deep lake environment (Zhang et al., 1998), which is a favorable condition for organic shale deposition (Lai et al., 2016). NMR logs were recorded in these reservoir, can be used to measure porosity and pore size distributions versus depth (Hossain et al., 2011; Lewis et al., 2013; Yu et al., 2017b). The new improved understanding of reservoirs will significantly aid exploitation as porosity and pore size distribution are the most important factors affecting transport behavior of fluids (Dullien, 2012; Kuila and Prasad, 2013; Tiab and Donaldson, 2015), hydrocarbon capability (Cai et al., 2013; Nie et al., 2015), elastic properties (Kockal and Ozturan, 2011; Sone and Zoback, 2013) and mechanical properties (Bandyopadhyay et al., 2010).

2.2. NMR well logging

Nuclear magnetic resonance (NMR) is a technique where hydrogen protons are magnetized (Coates et al., 1999) and the transverse relaxation time (T_1&T_2) of protons under the condition of pulsed and static magnetic fields is measured. This T_2 signal is directly proportional to the amount of hydrogen protons in the pore fluid (Kleinberg et al., 1994; Neto et al., 2009; Zhang et al., 2016). In conventional reservoirs, such as sandstone reservoirs, the NMR spectrum has generally 2 to 3 main peaks and the peaks get larger at higher relaxation time (Fig. 2a): the first smaller peak is normally clay bound water, the second peak is capillary bound water in small pores, and the third one is free water in large pores (Bauer et al., 2015; Yao et al., 2010). However, the shape of the T_2 distribution in shale gas reservoirs is totally different from that in sandstone (Fig. 2b). Here the first peak normally is the predominant one covering clay bound water and capillary bound water, while only some small peaks for free fluid volume and micro-fractures appear (Testamanti and Rezaee, 2017).

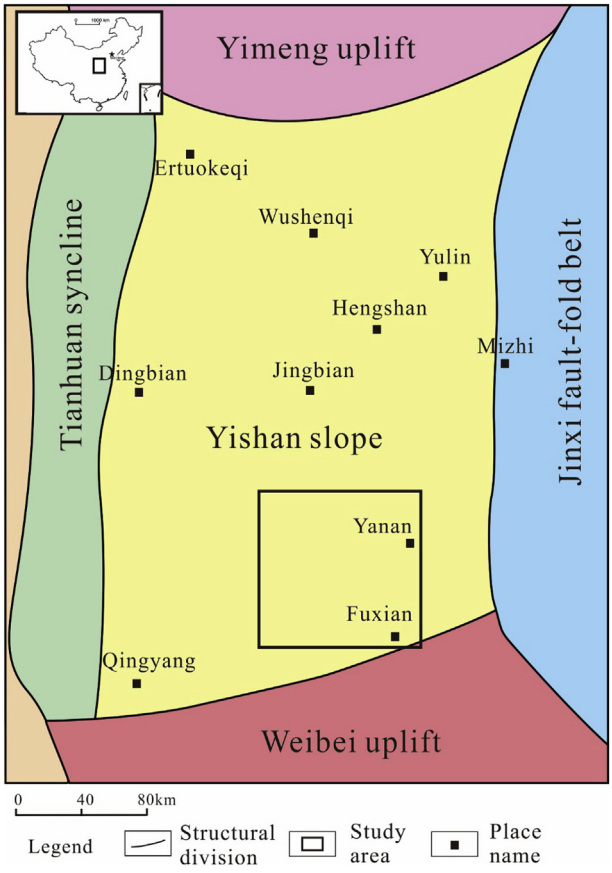

Fig. 1. Research area location map.

2.3. Pulsed-Neutron Spectrometry (PNS)

Pulsed-Neutron Spectrometry (PNS) log is a type of wireline log for detecting different elements in the formation (Wang and Carr, 2012). PNS measures relative elemental concentrationsaccording to neutron-induced gamma ray spectroscopy (Buller et al., 2010). PNS thus measures the primary elements, including silicon (Si),

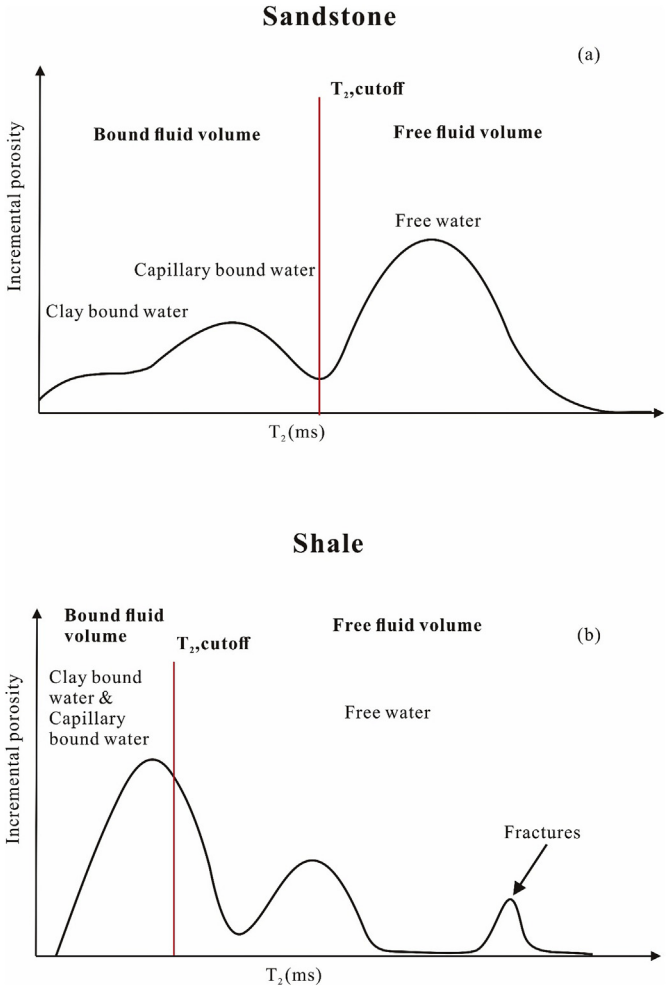

Fig. 2. A comparison between T_2 distribution for typical sandstone (a) and shale (b) reservoirs (Coates et al., 1999; Abouelresh, 2017).

calcium (Ca), titanium (Ti), barium (Ba), iron (Fe), gadolinium (Gd), sulfur (S), chlorine (Cl) and hydrogen (H).

2.4. Expectation Maximization clustering

Clustering is a machine learning method for grouping objects together where the variables are similar and different from other clusters (Jain, 2010; Perez, 2011). Expectation Maximization (EM) is one method for such clustering (Gupta and Chen, 2011). EM operates similar to the K-Means technique (Kou et al., 2014), where a fixed number of *k* clusters is given, and make sure the variables in one cluster havemaximize differencesto other clusters. The EM algorithm improved this basic approach in two essential ways (Na et al., 2010); (1) The EM clustering algorithm calculates probabilities of cluster memberships on the basis of one or more probability distribution. The goal of the clustering algorithm then is to maximize the overall probability or likelihood of the data, given the (final) clusters.(2) The conventional k-means clustering method only can be applied to discrete data. However, the EM algorithm can be used also for continuous and categorical variables.

3. Methods

The mineral compositions of the shale reservoir studied were obtained from the PNS logs. The oxide-closure model was applied forconverting relative elemental yields to weight percentage (Skelt, 2010; Wang et al., 2017). This model assumesthat the total of all oxides in the formation rock matrix is 100% and that all sedimentary minerals are oxides; therefore, the dry weight percent of all oxides in the rock matrix must be 100% (Harvey et al., 1992). Then, the weight percent of each oxide is interpreted from the cation weight percent with the mineral chemical formula, e.g. Si is main element in quartz, Ca has a closed relationship with dolomite and limestone, Fe can be used to calculate pyrite and Al is used to get the claycontent (Ward, 2002). Total organic carbon (TOC) can be calculated from well logs. We chose the method proposed in (Yu et al., 2017a) to obtain the TOC content.

We proposed a work flow for NMR clustering including six foundational steps as presented in Fig. 3 .

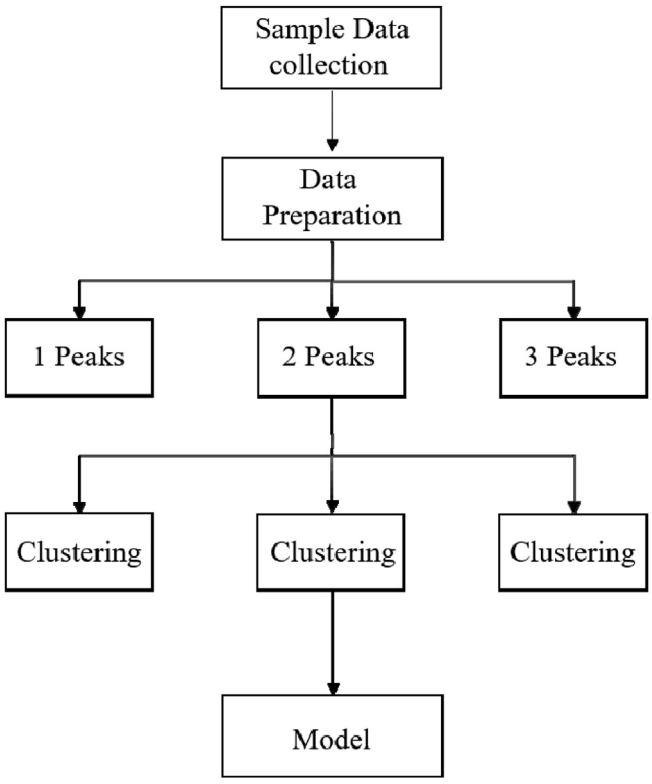

Fig. 3. Clustering flow chart.

(1) Initially all NMR spectra from available wells were collected.
(2) Data preparation decomposes the NMR spectra to normal dataset instead of curve. For the NMR spectrum, the relaxation time and amplitude of each peak is the key point in evaluating pore size distribution. Hence, we read the relaxation time and amplitude of each peak with Matlab. One example can be seen in Table 1. The dataset will be separated by the number of peaks as data with different number of peaks indicate different pore structures.

4. Results and discussion

4.1. T_2 distribution of NMR well logging

4.1.1. Pore size distribution in shale gas reservoir

The NMR log spectra show some noticeable variation with the depth (Fig. 7); this indicates that means different pore sizes are present in the studied shale formation. T_2 distribution curves were divided into 8 logarithmic equidistance ranges (i.e. 0.3 ms, 1 ms, 3 ms, 10 ms, 30 ms, 100 ms, 300 ms, 1000 ms and 3000 ms) to analyze pore size changes versus depth, e.g..Small size pores (e.g., clay bound water) take up a major part of the total porosity and the volume of pores decreases sharply with increasing the relaxation time, indicating that larger pores (e.g., free fluid pores) are not the major pore type in this shale gas reservoir.

4.1.2. Characteristics of NMR spectra

We found that most of the T_2 distributions shows thereor more peaks in the NMR log, which is not consistent with most earlier studies (Lewis et al., 2013; Odusina et al., 2011). Previous studies reported shale NMR spectrashowing only two peaks (Meng et al.,

Table 1
An example of data collected from T2 curve.
(3) Data clustering is accomplished via the EM algorithm. All T_2 curve variables thus are subdivided into subgroups with similar T_2 distribution shapes.
(4) Model is group clustering.
(5) In the Expert performance evaluationthe significance of the clustering results is evaluated by mineral composition and organic matter, combining NMR experiment on shale sample with fracture of fully saturated and after centrifuge which also from the same formation.

	Peak 1		Peak 2		Peak 3	
Peak numbers	Relaxation time	Amplitude	Relaxation time	Amplitude	Relaxation time	Amplitude
3	1.294321	0.004135091	15.53842	0.001857065	804.8087	0.000201686
3	1.294321	0.004183379	32.27508	0.001559834	1078.144	0.000109741
2	1.733908	0.003260394	50.04301	0.001686265		
2	2.322791	0.002431929	67.03901	0.002244825		
1	4.168487	0.00338517				
1	4.824702	0.003900562				

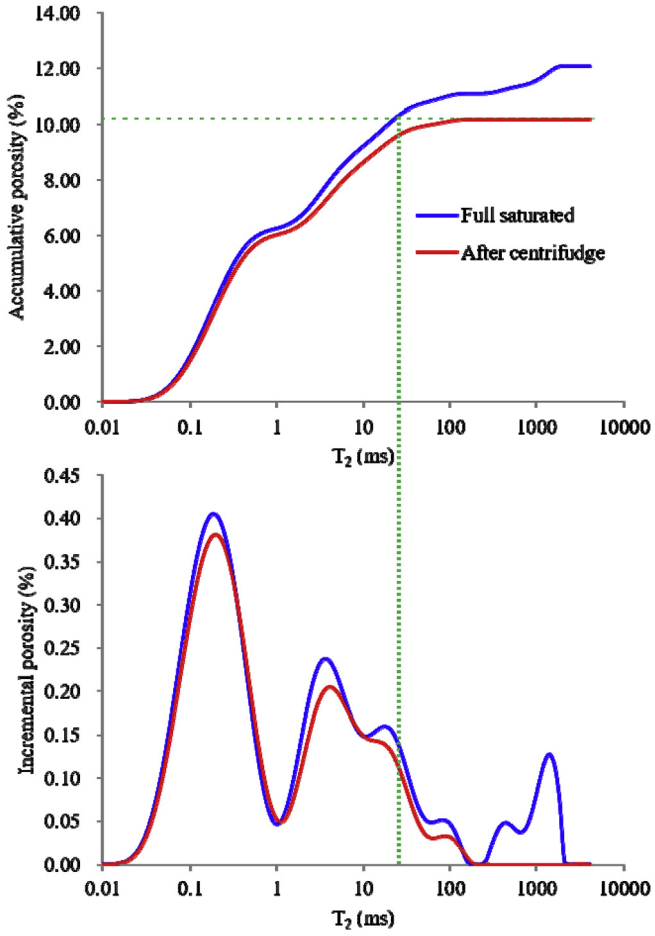

Fig. 4. Laboratory test T_2 spectra of the shale sample.

2016; Tinni et al., 2014). The morphology of the three peaksindicates that there are at least three types of pores existing in the shale gas reservoirbecause different peaks represent fluids exist in different pores. Thus we can indicate the fluids types by the peak and therefore the pore types are obtained. To investigate this further, we conducted a NMR laboratory experiment. In Fig. 5, the blue line is the T_2 spectrum of the fully brine saturated shale, while the red line shows the T_2 spectrum after 24 h centrifuging. The third peak disappeared after centrifuging, while the other two peaks slightly decreased. The third peak can be interpreted as a fracture, consistent with the presence of open cracks within the sample. Considering the accumulative porosity plot, we determined three $T_{2cutoff}$ (Fig. 4): (1) clay bound water (CBW) cutoff at about 0.7 ms; (2) the capillary and free fluid cutoff at 22 ms; and (3) fracture volume cutoff at 200 ms.

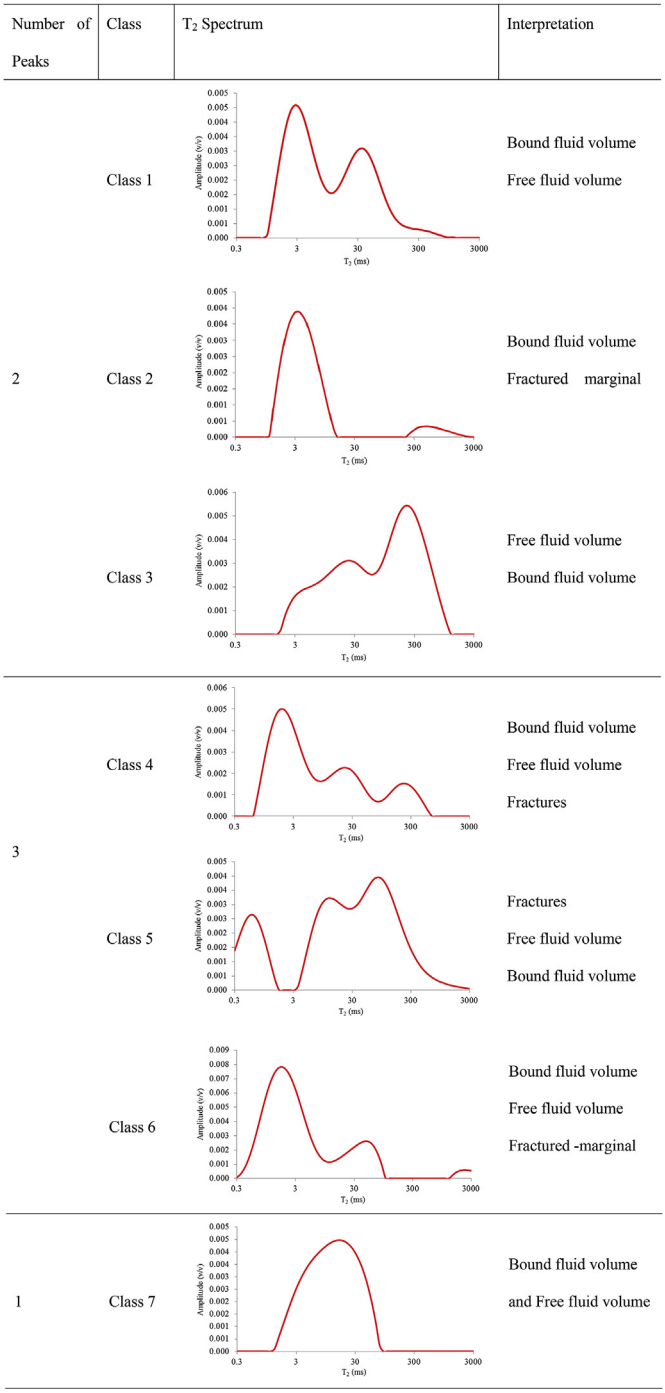

Fig. 5. Classification of representative NMR spectra.

4.2. Reservoir type and lithological group classification

Each curvature in an NMR graph reflects distinct pore distribution characteristics. Such characteristics can be interpreted for a specific lithofacies (Bauer et al., 2015; Yao et al., 2010). Our methodology is to identify a well-defined pore size distribution and mineral composition from the NMR curves which are representative of distinct reservoir and lithofaces types.

Data clustering conducted in three groups of 3 peaks, 2 peaks and 1 peak respectively. Then, different number of clusters was tried in each group. The results showed that when the number of the clusters is larger than 3 in the 3 peaks group and 2 peaks group, the additional clusters just have 0 data. Therefore, we concluded that 3 classes are the reasonable and ideal number in 3 peaks group and 2 peaks group, and only 1 class in the 1 peak group.

A total of 7 classes were obtained (Fig.s 6, 7 and Table 2), where each class is characterized by a distinct shape of the NMR T_2 distribution curves. The geological interpretation and evaluation of the 7 classes are illustrated on the basis of the shape of their NMR T_2 distribution curves (Fig. 6). The NMR T_2 distribution curves can reflect specific pore space distributions which are consistent with the mineral composition. Normally, high clay content indicate high clay bound water, inverse, high quartz and feldspar show more

Table 2
Composition statistics for the proposed NMR classes.

Class	Parameter	TOC (wt%)	Carbonate (fraction)	Clay (fraction)	Quartz + Feldspar (fraction)
1	Minimum	0.09	0.00	0.17	0.33
	Maximum	5.86	0.29	0.58	0.73
	Average	1.42	0.09	0.37	0.52
	Standard deviation	1.43	0.05	0.07	0.07
2	Minimum	0.11	0.00	0.16	0.36
	Maximum	5.34	0.32	0.58	0.71
	Average	1.26	0.10	0.36	0.51
	Standard deviation	1.44	0.06	0.08	0.06
3	Minimum	0.25	0.00	0.17	0.44
	Maximum	5.01	0.20	0.48	0.76
	Average	0.91	0.10	0.27	0.61
	Standard deviation	1	0.05	0.06	
4	Minimum	0.14	0.00	0.19	0.29
	Maximum	5.95	0.33	0.57	0.73
	Average	1.97	0.08	0.40	0.50
	Standard deviation	1.62	0.06	0.08	0.07
5	Minimum	0.19	0.00	0.17	0.41
	Maximum	4.12	0.27	0.49	0.80
	Average	0.78	0.11	0.28	0.60
	Standard deviation	0.89	0.05	0.07	0.08
6	Minimum	0.15	0.00	0.15	0.31
	Maximum	6.60	0.32	0.60	0.70
	Average	1.80	0.10	0.38	0.50
	Standard deviation	1.55	0.06	0.08	0.07
7	Minimum	0.17	0.00	0.19	0.40
	Maximum	5.15	0.25	0.44	0.69
	Average	0.86	0.09	0.32	0.58
	Standard deviation	1.03	0.06	0.06	0.07
Total	Minimum	0.09	0.00	0.15	0.29
	Maximum	6.60	0.33	0.60	0.80
	Average	1.51	0.09	0.36	0.52
	Standard deviation	1.48	0.06	0.08	0.08

fractures.

Class 1 is very common in shale gas reservoirs. Normally, in shale gas reservoir, the porosity of bound water is larger thanthat of free fluid (Testamanti and Rezaee, 2017). We can see that the TOC, clay, carbonate and quartz plus feldspar contents are all similar (Fig.s5, 6 and Table 2). This class is a typical sub-reservoir with high clay content and TOC, low clastic mineral content, and medium carbonate cementation.

Class 2 shows an amplitude peak around 3 ms and a minor peak at around 300 ms. Thus the volume of bound water is high and it is fractured. Interestingly there is no free water volume due to high carbonate cementation, and this is clarified by the carbonate content from PNS log. All mineral contents are similar to Class 1 except the content of quartz plus feldspar. Most sub-reservoirs in Class 2 have a lower quartz plus feldspar content when compared to Class 1; such mineral composition results in high bound water volume and low free fluid volume. This class is thus not favorable for free gas storage; however, due to its high TOC content, it is rock in absorbed gas.

Class 3 differs significantly from class 1 and class 2; a moderate elongated peak around 3–30 ms and a high peak around 100 ms appear here. This type of T_2 spectrum indicates that the fractures volume comprises most of the pore space, and free fluid volume and clay bound water volume overlap. Thus, this sub-reservoir type is one of the best reservoirs for shale gas storage and exploitation. It has the highest content of quartz plus feldspar (average value is 61.02 wt%, minimum value is 44.37 wt%) and lowest clay content (average 17.46 wt%, maximum value is 47.46 wt%).

Class 4 shows the highest bound water volume, low free fluid volume and a lower degree of fracturing. The mineral composition is similar to class 1.

Class 5 shows two peaks clearly at around 10 ms, 100 ms and a minor peak below 1 ms. Thus it contains high free fluid volume and capillary bound volume, and a small amount of clay bound water. It is also one of the best reservoir type, because it has a high free fluid volume.

Class 6 is similar to Class 4; although this group only has a few large fractures compared to many fractures in Class 4. However, these large fractures provide a good pathway for gas migration which is helpful during gas accumulation and shale gas extraction.

Class 7 is characterized by a single peak with a large amplitude around 2–60 ms (and only taking very small proportion in the NMR well logging data), indicating a large amount of free fluid volume and capillary bound volume, and no clay bound water.

The above 7 classes were divided only by data driven, however, sometimes, 7 classes were more complicated for geological evaluation. We thus categorized them as three lithofacies clusters (Fig. 7) based on TOC, clay, carbonate, and detrital contents of these seven classes, aimed at to access geological and exploitation evaluation.

Cluster 1 includes Class 1, Class 4 and Class 6. The first peak in Cluster 1 is the largest peak followed by a second peak, while the third peak is usually missing or it is insignificant. This indicates that the main pore types are micropores and meso/macro pores. The mineral composition in this cluster shows high TOC and clay content, and low carbonate and quartz and feldspar contents.

Cluster 2 only contains Class 2. The NMR spectrum of this cluster has one peak around 3 ms, illustrating that micropore prevail. The difference in composition between Cluster 1 and Cluster 2 is that Cluster 2 has a higher carbonate content. This could be because some meso/macro pores are cemented by carbonate.

Class 3, Class 5 and class 7 are categorized as Cluster 3. The NMR spectrum of Cluster 3 has an inverse shape when compared with Cluster 1. In this cluster the third peak is the largest peak followed by the second peaks, indicating that large pores and fractures are the main pore types. The low TOC and clay content can be verified this character. Although Cluster 3 has slightly higher carbonate

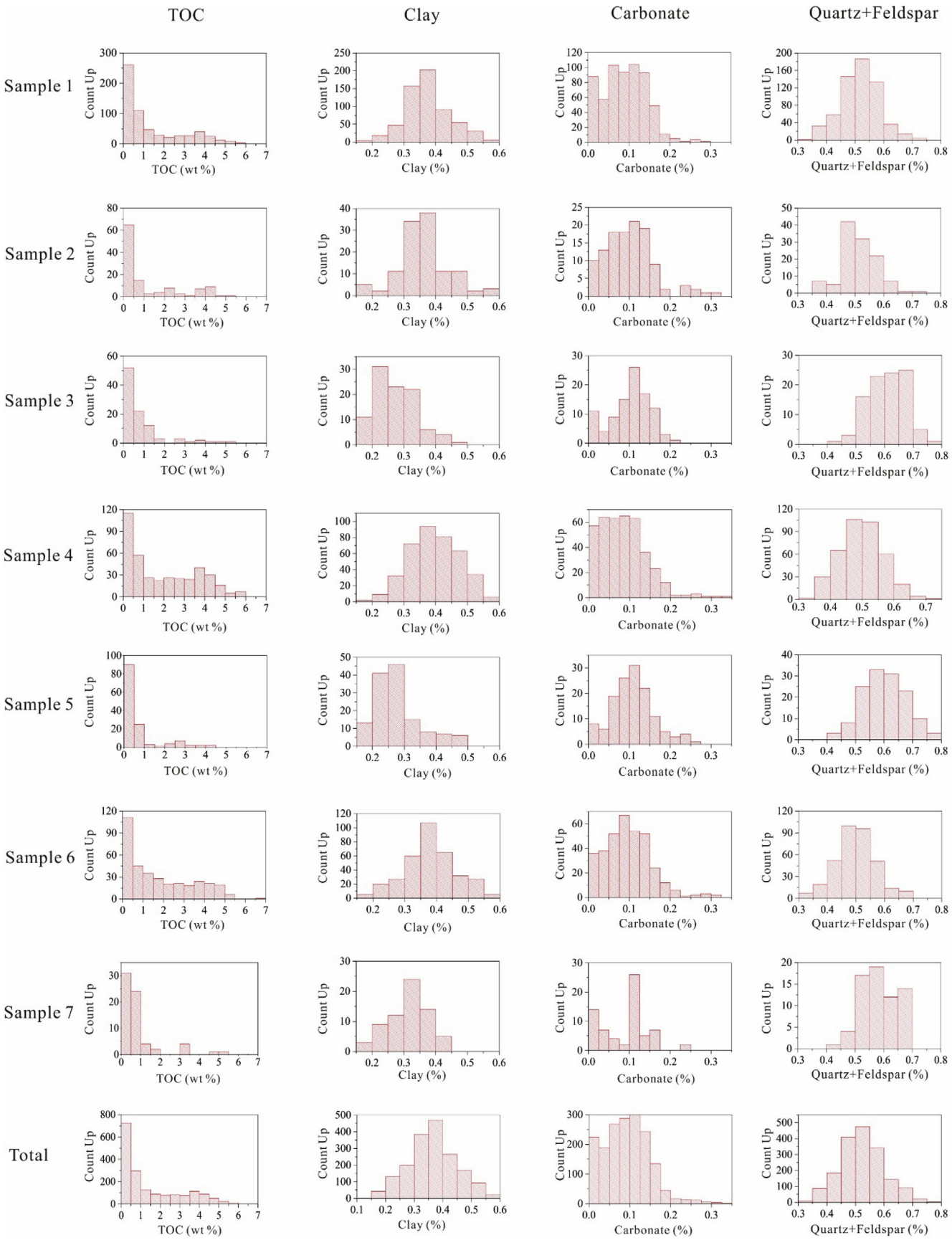

Fig. 6. Histogram showing TOC, clay, carbonate and quartz + feldspar for each NMR class.

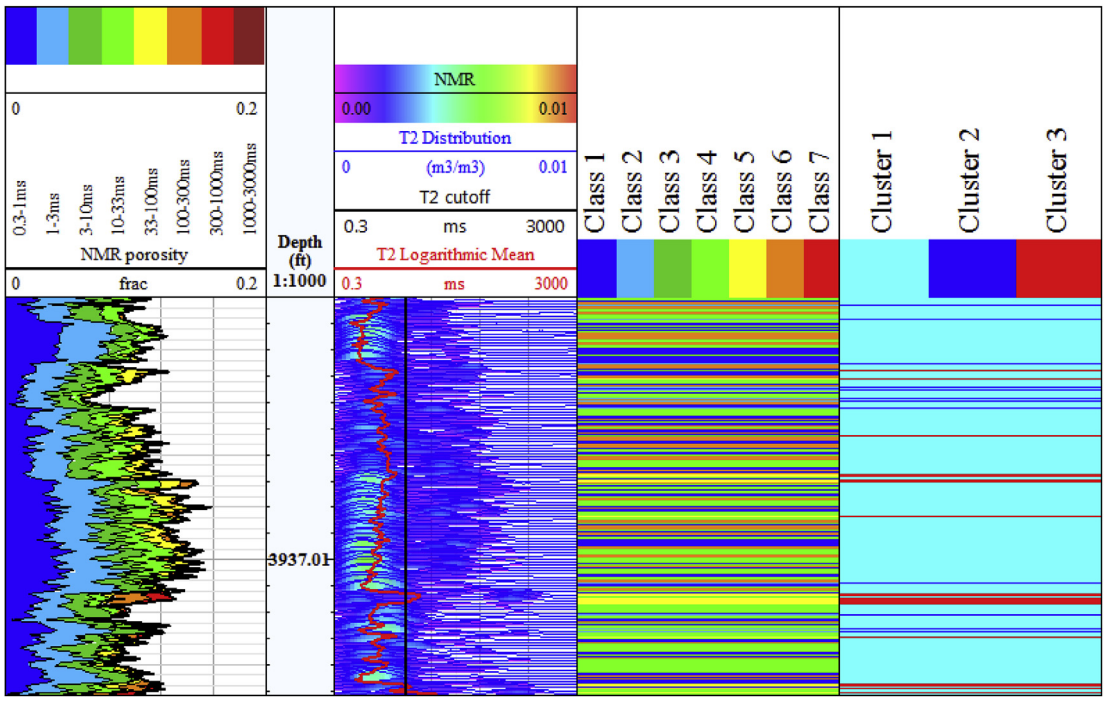

Fig. 7. The classification of classes and clusters using NMR log data.

content than Cluster 1, it has significantly higher quartz and feldspar content which has a strong influence on the pore size (Baruch et al., 2015).

4.3. Application

This color-coding NMR curve shows the distribution of different classes and clusters with depth (Fig. 7). Hydraulic fracturing design needs to know the brittleness of shale, which is determined by the content of quartz and feldspar. In our classification, Cluster 3 has a high quartz and feldspar content which results in the high percentage of large pores. High quartz and feldspar contents in shales normally develop many natural fractures as they are brittle and prone to be fractured during fracturing (Ding et al., 2012; Zhang et al., 2019; Yaghoubi, 2019; Gale et al., 2014). Rock heterogeneity is an important property in reservoir characterization and also hydraulic fracturing design (Suarez-Rivera et al., 2011; Tang et al., 2015). The pore type spectrum is related to the shale heterogeneity. More long relaxation components than short relaxation componentsindicate stronger shale heterogeneity (Zhao et al., 2017). Thus shale Cluster 3 is more heterogeneous, followed by Cluster 1 and Cluster 2. We thus believe that NMR spectra can be used toquantify the heterogeneity of the shale reservoir based on the peaks. This result can provide support for choosing the location and method of shale fracturing.

5. Conclusion

We analyzed T_2 spectra of NMR well log data to evaluate the pore structure and reservoir type of a shale reservoir. The pore size distribution changed with the depth. However, some of the T_2 relaxation times were >300 ms. We found that small pores (0.3 ms–1 ms and 1 ms–3 ms) comprised the major part of the porosity, while the larger pores (300 ms–1000 ms and 1000 ms–3000 ms) only accounted for a small porosity proportion. However, there always existed a third peak in the NMR spectrum, which disappeared after centrifuge. We thus conclude that the third peak are fractures in the shale gas reservoir, consistent with the centrifuging experiments (see section 4.2.1).

We also sorted the NMR spectra with a clustering method, an effective tool to classify lithological groups, based on relaxation time and the shape of NMR spectrum. A total of 7 reservoir classes were identified; these represent 7 sub-reservoirs in the shale formation. Further, we described these classes in terms of mineral composition from PNS well-log data. These different classes could again be lumped into 3 clusters, which can be used to evaluate fracturing and reservoir heterogeneity.

Finally, we conclude that NMR log data can be used to estimate reservoir zoning in shale gas reservoirs. These results thus could provide key geological and exploitation information for improved field development.

Acknowledgments

This work was jointly funded by National Natural Science Foundation of China (41902145), Natural Science Basic Research Plan in Shaanxi Province of China (2020JQ-594), Young Talent fund of University Association for Science and Technology in Shaanxi, China (20180701) and National and Local Joint Engineering Research Center for Carbon Capture Utilization and Sequestration at Northwest University in China. The measurements were performed using the μCT system of the National Geosequestration Laboratory (NGL) of Australia. Funding for the facilities was provided by the Australian Federal Government. This work was also supported by the Pawsey Supercomputing Centre, who provided the Avizo 9.5 image processing software and workstation, with funding from the Australian Government and the Government of Western Australia.

References

Abouelresh, M.O., 2017. An integrated characterization of the porosity in Qusaiba Shale, Saudi Arabia. J. Petrol. Sci. Eng. 149, 75–87.

Bandyopadhyay, A., Espana, F., Balla, V.K., Bose, S., Ohgami, Y., Davies, N.M., 2010. Influence of porosity on mechanical properties and in vivo response of Ti6al4v implants. Acta Biomater. 6, 1640–1648.
Baruch, E.T., Kennedy, M.J., Löhr, S.C., Dewhurst, D.N., 2015. Feldspar dissolution-enhanced porosity in paleoproterozoic shale reservoir facies from the barney creek formation (mcarthur basin, Australia). AAPG Bull. 99, 1745–1770.
Bauer, K., Kulenkampff, J., Henninges, J., Spangenberg, E., 2015. Lithological control on gas hydrate saturation as revealed by signal classification of Nmr logging data. J. Geophys. Res.: Solid Earth 120, 6001–6017.
Buller, D., Hughes, S.N., Market, J., Petre, J.E., Spain, D.R., Odumosu, T., 2010. Petrophysical evaluation for enhancing hydraulic stimulation in horizontal shale gas wells. In: Spe Annual Technical Conference and Exhibition. Society of Petroleum Engineers.
Cai, Y., Liu, D., Pan, Z., Yao, Y., Li, J., Qiu, Y., 2013. Pore structure and its impact on Ch4 adsorption capacity and flow capability of bituminous and subbituminous coals from Northeast China. Fuel 103, 258–268.
Chalmers, G.R., Bustin, R.M., Power, I.M., 2012. Characterization of gas shale pore systems by porosimetry, pycnometry, surface area, and field emission scanning electron microscopy/transmission electron microscopy image analyses: examples from the Barnett, Woodford, Haynesville, Marcellus, and Doig unitscharacterization of Gas Shale Pore Systems. AAPG Bull. 96, 1099–1119.
Cho, G., Wu, Y., Ackerman, J.L., 2003. Detection of hydroxyl ions in bone mineral by solid-state Nmr spectroscopy. Science 300, 1123–1127.
Coates, G.R., Xiao, L., Prammer, M.G., 1999. Nmr Logging: Principles and Applications. Haliburton Energy Services, Houston.
Ding, W., Li, C., Li, C., Xu, C., Jiu, K., Zeng, W., Wu, L., 2012. Fracture development in shale and its relationship to gas accumulation. Geoscience Frontiers 3, 97–105.
Dullien, F.A., 2012. Porous Media: Fluid Transport and Pore Structure. Academic Press.
Gale, J.F., Laubach, S.E., Olson, J.E., Eichhubl, P., Fall, A., 2014. Natural fractures in shale: a review and new observationsnatural fractures in shale: a review and new observations. AAPG Bull. 98, 2165–2216.
Gallegos, D.P., Smith, D.M., 1988. A Nmr technique for the analysis of pore structure: determination of continuous pore size distributions. J. Colloid Interface Sci. 122, 143–153.
Gupta, M.R., Chen, Y., 2011. Theory and use of the Em algorithm. Foundations and Trends® in Signal Processing 4, 223–296.
Harvey, P., Lofts, J., Lovell, M., 1992. Mineralogy Logs: Element to Mineral Transforms and Compositional Colinearity in Sediments. Spwla 33rd Annual Logging Symposium. Society of Petrophysicists and Well-Log Analysts.
Hongyan, Y., Li, W., Xiaoyan, Q., Zhenliang, W., Cheng, H., Aiguo, W., Dongxu, W., Qianghan, F., Yifei, L., Yong, W., 2016. Gas and water distribution of ordovician majiagou formation in northwest of Ordos Basin, nw China. Petrol. Explor. Dev. 43, 435–442.
Hossain, Z., Grattoni, C.A., Solymar, M., Fabricius, I.L., 2011. Petrophysical properties of greensand as predicted from Nmr measurements. Petrol. Geosci. 17, 111–125.
Howard, J., Kenyon, W., Morriss, C., Straley, C., 1995. Nmr in partially saturated rocks: laboratory insights on free fluid index and comparison with borehole logs. Log. Anal. 36.
Jain, A.K., 2010. Data clustering: 50 years beyond K-means. Pattern Recogn. Lett. 31, 651–666.
Kamath, S., Colby, R.H., Kumar, S.K., Karatasos, K., Floudas, G., Fytas, G., Roovers, J.E., 1999. Segmental dynamics of miscible polymer blends: comparison of the predictions of a concentration fluctuation model to experiment. J. Chem. Phys. 111, 6121–6128.
Kapur, G., Findeisen, M., Berger, S., 2000. Analysis of hydrocarbon mixtures by diffusion-ordered Nmr spectroscopy. Fuel 79, 1347–1351.
Kenyon, W., 1997. Petrophysical principles of applications of Nmr logging. Log. Anal. 38 (2).
Kleinberg, R., Flaum, C., Griffin, D., Brewer, P., Malby, G., Peltzer, E., Yesinowski, J., 2003. Deep sea Nmr: methane hydrate growth habit in porous media and its relationship to hydraulic permeability, deposit accumulation, and submarine slope stability. J. Geophys. Res.: Solid Earth 108 (B10).
Kleinberg, R., Kenyon, W., Mitra, P., 1994. Mechanism of Nmr relaxation of fluids in rock. J. Magn. Reson., Ser. A 108, 206–214.
Kockal, N.U., Ozturan, T., 2011. Strength and elastic properties of structural lightweight concretes. Mater. Des. 32, 2396–2403.
Kou, G., Peng, Y., Wang, G., 2014. Evaluation of clustering algorithms for financial risk analysis using Mcdm methods. Inf. Sci. 275, 1–12.
Kuila, U., Prasad, M., 2013. Specific surface area and pore-size distribution in clays and shales. Geophys. Prospect. 61, 341–362.
Lai, J., Wang, G., Ran, Y., Zhou, Z., Cui, Y., 2016. Impact of diagenesis on the reservoir quality of tight oil sandstones: the case of Upper Triassic Yanchang Formation Chang 7 oil layers in Ordos Basin, China. J. Petrol. Sci. Eng. 145, 54–65.
Latorraca, G., Dunn, K., Webber, P., Carison, R., Stonard, S., 1999. Heavy Oil Viscosity Determination Using Nmr Logs. Spwla 40th Annual Logging Symposium. Society of Petrophysicists and Well-Log Analysts.
Lewis, R., Singer, P., Jiang, T., Rylander, E., Sinclair, S., Mclin, R.H., 2013. Nmr T2 distributions in the Eagle Ford shale: reflections on pore size. In: Spe Unconventional Resources Conference-Usa. Society of Petroleum Engineers.
Liu, Z.B., Gao, B., Hu, Z.Q., Du, W., Nie, H.K., Jiang, T., 2018. Pore characteristics and formation mechanism of high-maturity organic-rich shale in Lower Cambrian Jiumenchong Formation, southern Guizhou. Petroleum Research 3 (1), 57–65.
Meng, M., Ge, H., Ji, W., Wang, X., 2016. Research on the auto-removal mechanism of shale aqueous phase trapping using low field nuclear magnetic resonance technique. J. Petrol. Sci. Eng. 137, 63–73.
Na, S., Xumin, L., Yong, G., 2010. Research on k-means clustering algorithm: an improved k-means clustering algorithm. In: 2010 Third International Symposium on Intelligent Information Technology and Security Informatics. Ieee, pp. 63–67.
Neto, A.C., Guinea, F., Peres, N.M., Novoselov, K.S., Geim, A.K., 2009. The electronic properties of graphene. Rev. Mod. Phys. 81, 109.
Nie, B., Liu, X., Yang, L., Meng, J., Li, X., 2015. Pore structure characterization of different rank coals using gas adsorption and scanning electron microscopy. Fuel 158, 908–917.
Odusina, E., Sigal, R.F., 2011. Laboratory Nmr measurements on methane saturated Barnett Shale samples. Petrophysics 52, 32–49.
Odusina, E.O., Sondergeld, C.H., Rai, C.S., 2011. Nmr Study of Shale Wettability. Canadian Unconventional Resources Conference. Society of Petroleum Engineers.
Pan, Y.-H., Sader, K., Powell, J.J., Bleloch, A., Gass, M., Trinick, J., Warley, A., Li, A., Brydson, R., Brown, A., 2009. 3d morphology of the human hepatic ferritin mineral core: new evidence for a subunit structure revealed by single particle analysis of Haadf-Stem images. J. Struct. Biol. 166, 22–31.
Perez, R., 2011. Application of Lmr and Clustering Analysis in Unconventional Reservoirs. Gtw Us Shales, Aapg.
Skelt, C., 2010. Petrophysical analysis of the green river formation, Southwestern Colorado-a case study in oil shale formation evaluation. In: Spwla 51st Annual Logging Symposium. Society of Petrophysicists and Well-Log Analysts.
Sone, H., Zoback, M.D., 2013. Mechanical properties of shale-gas reservoir rocks—Part 1: static and dynamic elastic properties and anisotropy. Geophysics 78, D381–D392.
Suarez-Rivera, R., Deenadayalu, C., Chertov, M., Hartanto, R.N., Gathogo, P., Kunjir, R., 2011. Improving horizontal completions on heterogeneous tight-shales. In: Canadian Unconventional Resources Conference. Society of Petroleum Engineers.
Talabi, O., Alsayari, S., Iglauer, S., Blunt, M.J., 2009. Pore-scale simulation of Nmr response. J. Petrol. Sci. Eng. 67, 168–178.
Tang, X., Jiang, Z., Li, Z., Gao, Z., Bai, Y., Zhao, S., Feng, J., 2015. The effect of the variation in material composition on the heterogeneous pore structure of high-maturity shale of the Silurian Longmaxi formation in the southeastern Sichuan Basin, China. J. Nat. Gas Sci. Eng. 23, 464–473.
Testamanti, M.N., Rezaee, R., 2017. Determination of Nmr T2 cut-off for clay bound water in shales: a case study of Carynginia Formation, Perth Basin, Western Australia. J. Petrol. Sci. Eng. 149, 497–503.
Tiab, D., Donaldson, E.C., 2015. Petrophysics: Theory and Practice of Measuring Reservoir Rock and Fluid Transport Properties. Gulf professional publishing.
Tinni, A., Odusina, E., Sulucarnain, I., Sondergeld, C., Rai, C., 2014. Nmr response of brine, oil and methane in organic rich shales. In: Spe Unconventional Resources Conference. Society of Petroleum Engineers.
Wang, G., Carr, T.R., 2012. Marcellus shale lithofacies prediction by multiclass neural network classification in the Appalachian Basin. Math. Geosci. 44, 975–1004.
Wang, S., Xiao, L., Yue, A., Wang, H., Liu, W., Fan, Y., 2017. Accurate inversion of elemental concentrations from the pulsed neutron geochemical logging based on an active-set method. J. Petrol. Sci. Eng. 157, 833–841.
Wang, Z.G., 2018. Reservoir forming conditions and key exploration and development technologies for marine shale gas fields in Fuling area, South China. Petroleum Research 3 (3), 197–209.
Ward, C.R., 2002. Analysis and significance of mineral matter in coal seams. Int. J. Coal Geol. 50, 135–168.
Yaghoubi, A., 2019. Hydraulic fracturing modeling using a discrete fracture network in the Barnett Shale. Int. J. Rock Mech. Min. Sci. 119, 98–108.
Yao, Y., Liu, D., 2012. Comparison of low-field Nmr and mercury intrusion porosimetry in characterizing pore size distributions of coals. Fuel 95, 152–158.
Yao, Y., Liu, D., Che, Y., Tang, D., Tang, S., Huang, W., 2010. Petrophysical characterization of coals by low-field nuclear magnetic resonance (Nmr). Fuel 89, 1371–1380.
Yu, H., Rezaee, R., Wang, Z., Han, T., Zhang, Y., Arif, M., Johnson, L., 2017a. A new method for Toc estimation in tight shale gas reservoirs. Int. J. Coal Geol. 179, 269–277.
Yu, H., Wang, Z., Rezaee, R., Arif, M., Xiao, L., 2016. Characterization of elastic properties of lacustrine shale reservoir using well logging and core analysis. In: Spe Asia Pacific Oil & Gas Conference and Exhibition. Society of Petroleum Engineers.
Yu, H., Wang, Z., Rezaee, R., Su, Y., Tan, W., Yuan, Y., Zhang, Y., Xiao, L., Liu, X., 2017b. Applications of nuclear magnetic resonance (Nmr) logs in shale gas reservoirs for pore size distribution evaluation. In: Unconventional Resources Technology Conference (Urtec).
Zhang, Y., He, Z., Jiang, S., Lu, S., Xiao, D., Chen, G., Li, Y., 2019. Fracture types in the lower Cambrian shale and their effect on shale gas accumulation, Upper Yangtze. Mar. Petrol. Geol. 99, 282–291.
Zhang, Y., Sarmadivaleh, M., Lebedev, M., Barifcani, A., Rezaee, R., Testamantia, N., Iglauer, S., 2016. Geo-mechanical weakening of limestone due to supercritical Co 2 injection. In: Offshore Technology Conference Asia (Offshore Technology Conference).
Zhang, Y.Q., Mercier, J.L., Vergély, P., 1998. Extension in the graben systems around the Ordos (China), and its contribution to the extrusion tectonics of south China with respect to Gobi-Mongolia. Tectonophysics 285, 41–75.
Zhao, P., Wang, Z., Sun, Z., Cai, J., Wang, L., 2017. Investigation on the pore structure and multifractal characteristics of tight oil reservoirs using Nmr measurements: permian Lucaogou Formation in Jimusaer Sag, Junggar Basin. Mar. Petrol. Geol. 86, 1067–1081.